JAM-A regulates permeability and inflammation in the intestine in vivo

Mike G. Laukoetter,[1,3] Porfirio Nava,[1] Winston Y. Lee,[1] Eric A. Severson,[1] Christopher T. Capaldo,[1] Brian A. Babbin,[1] Ifor R. Williams,[1] Michael Koval,[2] Eric Peatman,[1] Jacquelyn A. Campbell,[4] Terence S. Dermody,[4,5] Asma Nusrat,[1] and Charles A. Parkos[1]

[1]Epithelial Pathobiology Research Unit, Department of Pathology and [2]Division of Pulmonary and Critical Care, Department of Medicine, Emory University, Atlanta, GA 30322
[3]Deparment of General Surgery, University of Muenster, 48149 Muenster, Germany
[4]Department of Microbiology and Immunology and Pediatrics and [5]Elizabeth B. Lamb Center for Pediatric Research, Vanderbilt University, Nashville, TN 37232

Recent evidence has linked intestinal permeability to mucosal inflammation, but molecular studies are lacking. Candidate regulatory molecules localized within the tight junction (TJ) include Junctional Adhesion Molecule (JAM-A), which has been implicated in the regulation of barrier function and leukocyte migration. Thus, we analyzed the intestinal mucosa of JAM-A–deficient (JAM-A$^{-/-}$) mice for evidence of enhanced permeability and inflammation. Colonic mucosa from JAM-A$^{-/-}$ mice had normal epithelial architecture but increased polymorphonuclear leukocyte infiltration and large lymphoid aggregates not seen in wild-type controls. Barrier function experiments revealed increased mucosal permeability, as indicated by enhanced dextran flux, and decreased transepithelial electrical resistance in JAM-A$^{-/-}$ mice. The in vivo observations were epithelial specific, because monolayers of JAM-A$^{-/-}$ epithelial cells also demonstrated increased permeability. Analyses of other TJ components revealed increased expression of claudin-10 and -15 in the colonic mucosa of JAM-A$^{-/-}$ mice and in JAM-A small interfering RNA–treated epithelial cells. Given the observed increase in colonic inflammation and permeability, we assessed the susceptibility of JAM-A$^{-/-}$ mice to the induction of colitis with dextran sulfate sodium (DSS). Although DSS-treated JAM-A$^{-/-}$ animals had increased clinical disease compared with controls, colonic mucosa showed less injury and increased epithelial proliferation. These findings demonstrate a complex role of JAM-A in intestinal homeostasis by regulating epithelial permeability, inflammation, and proliferation.

CORRESPONDENCE
Charles A. Parkos:
cparkos@emory.edu
OR
Asma Nusrat:
anusrat@emory.edu

Increased intestinal epithelial permeability and luminal antigen leakage across the barrier has been linked to chronic mucosal inflammation and inflammatory bowel disease (IBD) in animals and humans. In certain mouse models of IBD, including Samp-Yit (1), enhanced permeability has been shown to predate the onset of intestinal inflammation. In humans, the two most common forms of IBD, Crohn's disease and ulcerative colitis, have been linked to an abnormal cell-mediated immune reaction to enteric bacterial antigens in genetically susceptible hosts (2) with enhanced mucosal permeability (3, 4). Thus, there is strong evidence for a link between the regulation of paracellular permeability and intestinal inflammation.

M.G. Laukoetter and P. Nava contributed equally to this work.

Paracellular permeability is regulated by the apical most intercellular junction referred to as the tight junction (TJ), which functions as a semipermeable gate to regulate passive movement of luminal fluid and molecules between epithelial cells. The molecular composition of the TJs is complex, consisting of multiple transmembrane proteins including claudin family members, occludin, and members of the Junctional Adhesion Molecule (JAM) protein family. Of the JAM family members, several studies have implicated JAM-A in the regulation of barrier function and the inflammatory response. This single-pass transmembrane protein is expressed in several cell types but is particularly abundant in epithelial and endothelial cells, where it accumulates at TJs (5).

Although unifying mechanistic studies are lacking, JAM-A has been reported to influence

The Journal of Experimental Medicine

several cellular processes, including regulation of paracellular permeability, cell polarity, cell adhesion, cell migration, angiogenesis, and leukocyte migration (6–10). We previously reported in vitro evidence of a role for JAM-A in the regulation of epithelial barrier function by demonstrating enhanced permeability to dextran and decreased transepithelial electrical resistance (TER) after JAM-A knockdown (8). Detailed in vivo permeability studies in JAM-A–deficient (JAM-A$^{-/-}$) mice are lacking, although there is one report of enhanced corneal permeability in JAM-A$^{-/-}$ animals (11).

Because it is not known whether JAM-A plays a direct role in the regulation of epithelial permeability and the mucosal inflammatory response, we performed a series of in vivo and in vitro experiments using JAM-A$^{-/-}$ mice and cultured human intestinal epithelial cells. In this report, we show that JAM-A deficiency results in increased colonic inflammation and paracellular permeability in parallel with altered expression of claudin-10 and -15, both of which regulate TJ barrier function (12) by formation of ion-selective pores composed of homo- and heterooligomers (13–15). We also report that JAM-A$^{-/-}$ mice have increased susceptibility to experimentally induced colitis in conjunction with enhanced epithelial proliferation.

RESULTS AND DISCUSSION

JAM-A deficiency in mice results in enhanced colonic inflammation

A widely accepted hypothesis as to the mechanism of chronic relapsing intestinal inflammation in IBD is that gut epithelial barrier dysfunction permits luminal antigens to enter the subepithelial tissues, resulting in the recruitment and activation of leukocytes. Because JAM-A has been implicated in both the regulation of barrier function and leukocyte recruitment, we performed histological analyses of colonic mucosa from JAM-A$^{-/-}$ mice to determine if there was evidence of increased inflammation, presumably in response to altered barrier function. Despite having normal epithelial architecture, JAM-A$^{-/-}$ mice had significantly increased small (30 vs. 7 aggregates <1 mm in JAM-A$^{-/-}$ vs. control (WT littermate) mice, respectively; Fig. 1 A) and large (5 vs. 0 aggregates ≥1 mm in JAM-A$^{-/-}$ vs. control mice, respectively; Fig. 1 B) lymphoid aggregates in the distal colon (three sections per mouse; $n = 7$ mice; $P < 0.05$).

As shown in Fig. 1 B, the lymphoid structures contained mostly B lymphocytes marking for B220 PE and T cells marking for Thy 1.2 APCs that were mostly CD4$^+$ (not depicted), which was consistent with isolated lymphoid follicles. Of note, many large isolated lymphoid follicles were localized below the muscularis mucosae (Fig. 1 C), which was not seen in any WT mice. These lymphoid aggregates contained abundant B cells (B220 PE) and DCs (CD11c). Examination of small intestines from JAM-A$^{-/-}$ and WT animals revealed no significant differences in the numbers of isolated lymphoid follicles or histology between the groups (unpublished data). Flow cytometric analyses of leukocytes derived from the mesenteric lymph nodes and spleen were performed to determine if there were differences in T cell, monocyte, or DC activation between JAM-A$^{-/-}$ and WT controls. No differences were observed in the frequencies of nonactivated T cells expressing low levels of CD44 and CD69 and high levels of CD62L. In addition, no differences in the expression patterns of the co-stimulation markers CD40 and CD80 and I-Ab were observed in populations of CD11b$^+$ and CD11c$^+$ cells (unpublished data). Given the reports of JAM protein–mediated regulation of permeability, we reasoned that these histologic findings could be secondary to increased local immune cell activation from luminal antigens driving the isolated lymphoid follicle hyperplasia within the colonic mucosa of JAM-A$^{-/-}$ mice. This appears to be a process localized to colonic mucosa, because we did not observe activation within systemic lymphoid tissues.

Because PMN infiltration could be expected under conditions of increased mucosal permeability to luminal contents, we assayed the colonic mucosa of JAM-A$^{-/-}$ and WT mice for evidence of acute inflammation. As shown in Fig. 1 D, a representative mucosal section demonstrated increased numbers of LY-6G–staining PMN (16) in the subepithelial lamina propria in JAM-A$^{-/-}$ mice compared with WT littermate controls ($n = 6$). No crypt abscesses were observed. Consistent with the LY-6G staining results, myeloperoxidase (MPO) activity of colonic mucosa was significantly increased in JAM-A$^{-/-}$ mice versus controls ($n = 6$; Fig. 1 E). These findings demonstrate increased infiltration of acute inflammatory cells in the colonic mucosa of JAM-A$^{-/-}$ mice.

Interestingly, JAM-A$^{-/-}$ mice have been reported to have reduced PMN and increased monocyte infiltration of tissues after ischemic injury (17) that was not seen in mice with endothelial-specific loss of JAM-A, suggesting that leukocyte-expressed JAM-A may play a role in PMN recruitment. On the contrary, our findings demonstrate elevated PMN infiltration of colonic mucosa in JAM-A$^{-/-}$ mice, which would be consistent with the enhanced recruitment of leukocytes caused by leakage of luminal chemoattractants across a more permeable epithelium.

JAM-A regulates intestinal mucosal permeability in vivo

Given the increased colonic inflammation noted in JAM-A$^{-/-}$ mice, we performed experiments to determine if there was increased mucosal permeability. Consistent with previous in vitro studies suggesting a role of JAM-A in the regulation of epithelial and endothelial permeability (5, 8, 18), small interfering RNA (siRNA)–mediated knockdown of JAM-A protein in human SK-CO15 colonic epithelial cells decreased TER (~60% decrease; $P < 0.05$; Fig. 2 A) compared with controls. We next performed in vivo experiments assessing gut barrier function in JAM-A$^{-/-}$. Initial physiologic experiments demonstrated enhanced permeability to ingested labeled dextran. As shown in Fig. 2 B, gastrointestinal permeability, as determined by serum FITC-dextran concentration (ng/ml) 4 h after gavage, was markedly increased in JAM-A$^{-/-}$ mice compared with controls ($n = 6$

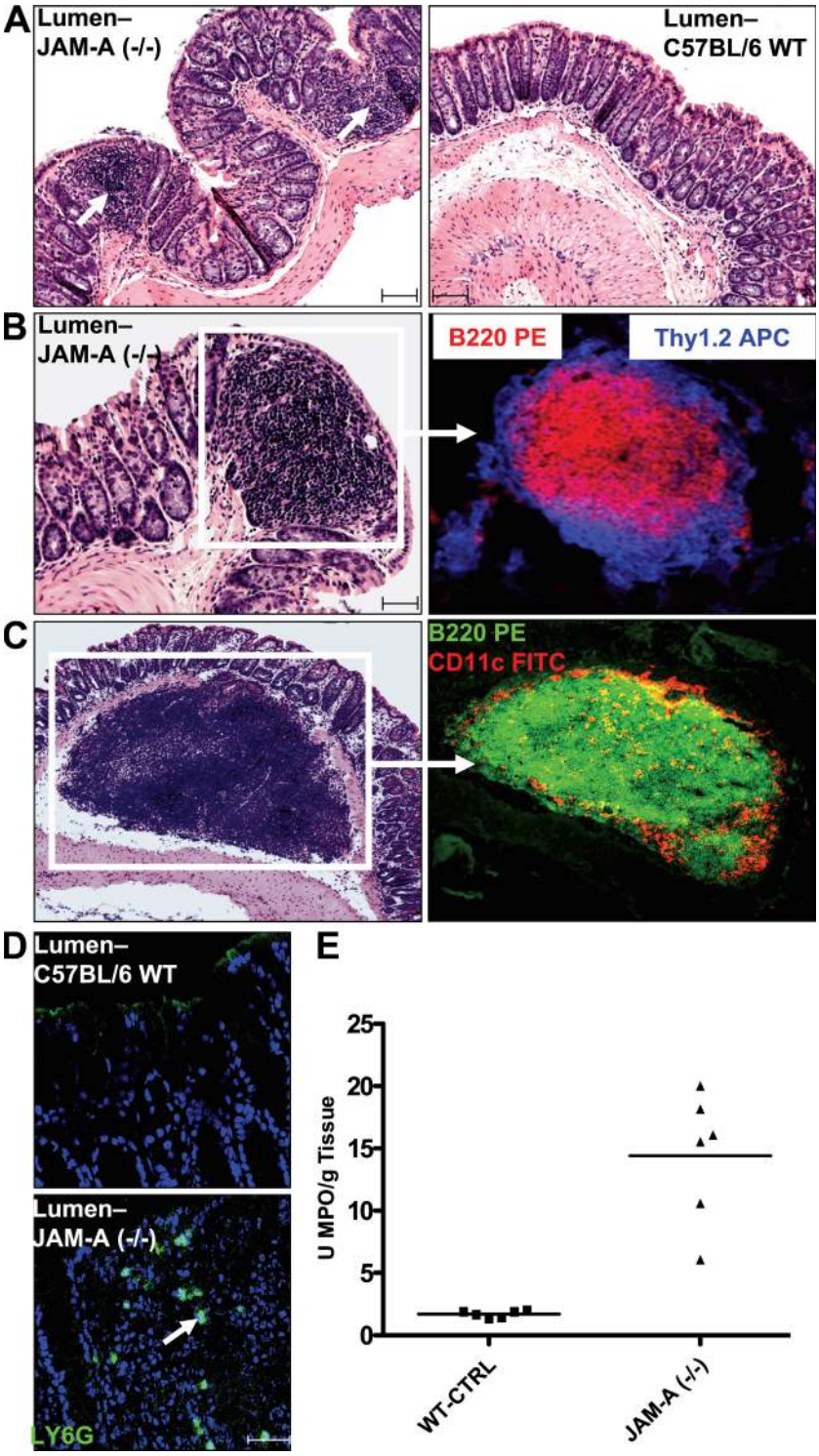

Figure 1. Increased colonic inflammation in JAM-A$^{-/-}$ mice. (A) Increased small lymphoid aggregates in JAM-A$^{-/-}$ mice. (B) Large lymphoid aggregates in JAM-A$^{-/-}$ mice identified as isolated lymphoid follicles. (C) Large, isolated submucosal lymphoid follicles observed only in JAM-A$^{-/-}$ mice. CD11c staining is shown in red. (D) Increased PMN in the colonic mucosa of JAM-A$^{-/-}$ mice. Bars, 40 μm. (E) MPO activity in the colonic mucosa of JAM-A$^{-/-}$ mice and littermate controls (n = 6). Horizontal bars represent the mean.

animals per condition). To better define the barrier defect, we next performed ex vivo permeability studies on colonic mucosa mounted in Ussing chambers. As shown in Fig. 2 C, there was increased flux of FITC-dextran (2 vs. 0.25 μg/h/cm^2) across the colonic mucosa of JAM-A$^{-/-}$ mice (n = 5 mice per condition; $P < 0.05$). In parallel, there was also decreased TER (Fig. 2 D) in mucosal tissue samples of JAM-A$^{-/-}$ mice compared with controls. Interestingly, we did not observe enhanced translocation of bacteria to the mesenteric lymph nodes and spleen in JAM-A$^{-/-}$ mice compared with controls (unpublished data), suggesting that the permeability defect is not sufficient to afford increased translocation of bacteria while permitting passage of smaller molecules. In addition, the absence of increased bacterial translocation in JAM-A$^{-/-}$ mice is consistent with our observation of a lack of systemic immune activation. These data thus provide direct evidence of JAM-A regulation of intestinal mucosal permeability in vivo. Indeed, the results of other studies with JAM-A$^{-/-}$ mice can be interpreted to support our findings. Cera et al. reported enhanced immune responses to antigens painted on the skin of JAM-A$^{-/-}$ mice secondary to the enhanced motility of DCs (10). However, the possibility of increased antigen exposure secondary to a leaky skin barrier was not addressed. In addition, Kang et al. recently reported that corneal epithelial permeability in JAM-A$^{-/-}$ animals is increased (11). Collectively, these data suggest a central role of JAM-A in the regulation of the epithelial barrier in vivo.

JAM-A deficiency results in enhanced expression of claudin-10 and -15 in vitro and in vivo

Because TJs regulate intestinal epithelial permeability, we examined whether the loss of JAM-A resulted in altered expression of TJ structural proteins. Although JAM-A per se has not been shown to directly form a selective barrier in transfected cells, recent studies have implicated a direct role of claudin proteins in regulating TJ permeability to water and ions (19–21). We thus assessed if the loss of JAM-A was associated with altered claudin expression. Monolayers of SK-CO15 cells were transfected with siRNA specific for JAM-A or control siRNA and surveyed for the altered expression of claudins. As shown in Fig. 3 A, Western blots of cells treated with JAM-A siRNA, but not lamin A/C or scramble controls, showed a 70–90% reduction in JAM-A protein along with significant up-regulation of claudin-10 and -15 and no change in occludin or claudin-2 levels. These findings show a role for JAM-A in the regulation of claudin expression.

To verify the physiologic relevance of the in vitro findings, we analyzed the protein levels of claudin-10 and -15 in distal colonic mucosal samples from JAM-A$^{-/-}$ mice. Consistent with the findings in Fig. 3 A, Western blots of colonic mucosal epithelial cell lysates from JAM-A$^{-/-}$ mice showed significant up-regulation of claudin-10 and -15 compared with controls, with no change in occludin or claudin-2 (Fig. 3 B). Densitometric analyses revealed 3.5- and 7.5-fold up-regulation of expression of claudin-10 and -15, respectively (Fig. 3 C). As shown in Fig. 3 (D–G), immunofluorescence analyses of

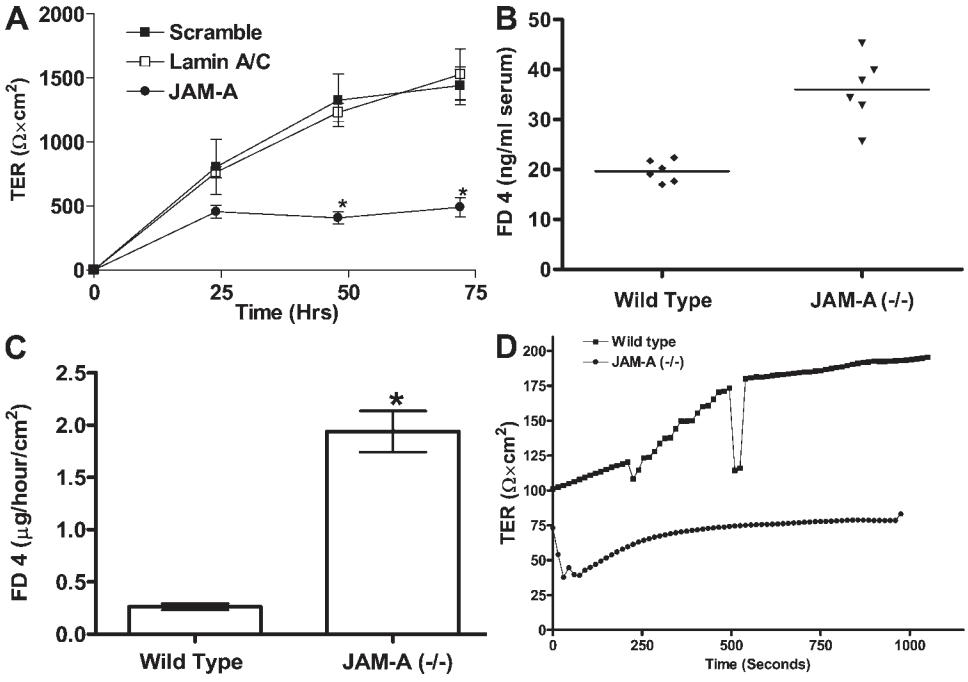

Figure 2. JAM-A deficiency results in enhanced intestinal permeability in vivo and in vitro. (A) TER of SK-CO15 cells after transient transfection with JAM-A siRNA. *, $P < 0.05$. (B) In vivo gastrointestinal permeability in control and JAM-A$^{-/-}$ mice 4 h after FITC-dextran gavage. Horizontal bars represent mean. (C) FD-4 flux across colonic mucosal sheets of WT and JAM-A$^{-/-}$ mice (n = 5 each). *, $P < 0.05$. Error bars in A and C represent the mean ± SEM. (D) Resistance across colonic mucosal sheets for JAM-A$^{-/-}$ mice and WT littermate controls (n = 5).

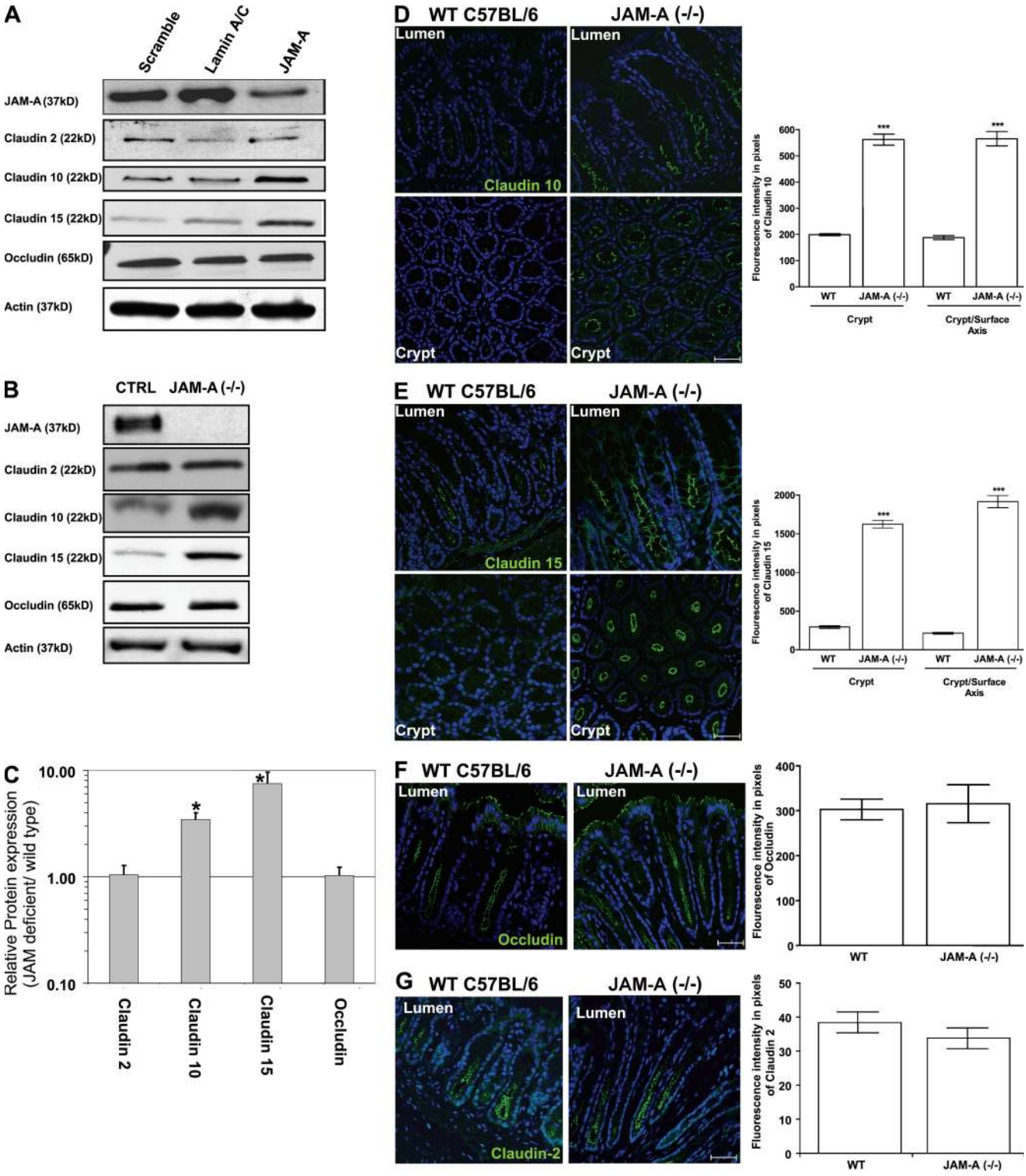

Figure 3. JAM-A deficiency results in altered claudin expression in vitro and in vivo. (A) Claudin protein expression profiles after JAM-A siRNA transfection in vitro. (B) Colonic mucosal claudin protein expression profiles in vivo from JAM-A$^{-/-}$ mice. (C) Densitometric analysis of claudin and occludin expression from Western blots obtained from WT and JAM-A$^{-/-}$ mice (n = 5 each). *, $P < 0.05$. (D–G) Immunofluorescence images of claudin-10 and -15, occludin, and claudin-2 expression in the colonic mucosa of WT and JAM-A$^{-/-}$ mice. ***, $P < 0.0001$. Error bars represent the mean ± SEM. Bars, 40 μM.

claudin expression in adjacent colonic mucosal sections from JAM-A$^{-/-}$ mice and controls performed at equivalent intensity/gain levels confirmed significant up-regulation of claudin-10 and -15 expression within the crypt epithelium in JAM-A$^{-/-}$ mice, with no change in the levels of claudin-2 or occludin compared with controls. Similar increases in claudin-10 and -15 were observed in the colonic mucosa of dextran sulfate sodium (DSS)–treated JAM-A$^{-/-}$ mice compared with DSS-treated WT controls (unpublished data).

Interestingly, claudin-10 and -15 have been reported to form a "leaky" barrier in certain tissues (19, 20), which is consistent with our observations of increased permeability and claudin expression in JAM-A$^{-/-}$ mice. Thus, we propose that the altered claudin expression observed may confer the increase in permeability of colonic mucosa in JAM-A$^{-/-}$ mice. Indeed, it is well documented that alterations in the ratios of claudins expressed by epithelial cells can have dramatic effects on the permeability to small molecules (12, 21). In this paper and a previous one, we observed no changes in the levels of other apical junctional complex proteins, such as occludin, zonula occludens 1, and E-cadherin, after loss of JAM-A expression (8). We speculate that the permeability defect observed is caused by changes in the claudin expression within TJ and not to gross changes in structure or assembly. Despite these observations, the cell-biological mechanism by which JAM-A mediates such changes in claudin protein levels remains to be determined. However, our findings suggest that complex regulation of protein expression may be involved, perhaps at the transcriptional level. These data demonstrate a mechanism for JAM-A–mediated regulation of epithelial paracellular permeability in vivo and a plausible link to regulation of inflammation and luminal antigen exposure.

Increased susceptibility to inflammation in JAM-A$^{-/-}$ mice challenged with DSS

We found it surprising that the JAM-A$^{-/-}$ animals had evidence of a B cell–rich isolated lymphoid follicle hyperplasia and increased permeability without any clinical evidence of colitis. Indeed, others have recently demonstrated an important role of B cell populations in triggering and potentiating IBD in mice (22, 23). These findings led us to predict that JAM-A$^{-/-}$ mice would have enhanced susceptibility to experimentally induced colitis. We thus used a well-established model of acute colitis using DSS (24) in JAM-A$^{-/-}$ mice and WT littermates. Mice ($n \geq 7$) were supplemented with 5% DSS in the drinking water for 7 d. All mice survived until their time of death, and drinking volume was similar (unpublished data). As shown in Fig. 4 (A and B), DSS-treated JAM-A$^{-/-}$ mice had significantly increased disease activity index (DAI) and decreased body weight compared with controls ($P < 0.05$). Furthermore, DSS-treated JAM-A$^{-/-}$ mice had increased colonic shortening ($P < 0.05$; Fig. 4 C) and fecal blood loss (not depicted) compared with controls. As expected, DSS treatment increased MPO activity in the colons of JAM-A$^{-/-}$ mice compared with controls receiving water alone (Fig. 4 D). Furthermore, MPO activity correlated closely with clinical and morphologic grading of inflammation in experimental groups. Interestingly, DSS-induced colonic MPO activity in JAM-A$^{-/-}$ mice, although increased compared with non–DSS-treated mice, was less than that in DSS-treated WT animals. A possible explanation includes desensitization of PMN because of enhanced exposure to microbial products in a more permeable mucosa. Alternatively, there may simply be a decreased availability of PMN for migration into the gut because of increased baseline PMN recruitment into tissues, as evident in Fig. 1 (D and E). Lastly, as others have proposed, there may be leukocyte-specific effects of JAM-A that affect recruitment.

By standard blinded histological scoring parameters, the colonic mucosa of control mice had minimal inflammation (Fig. 4 E), however, DSS treatment resulted in a markedly increased score (Fig. 4 E). In WT C57BL/6 littermates, inflammation was mainly confined to the mucosa with a loss of goblet cells, crypt damage, prominent mucosal ulceration, and edema (Fig. 4 F). Surprisingly, despite worse clinical scores, DSS-treated JAM-A$^{-/-}$ mice showed less severe injury and less edema than controls (2.66 ± 0.943 [SD] vs. 4.04 ± 0.68 [SD] for JAM-A$^{-/-}$ vs. WT controls, respectively; $P < 0.007$). Reduced edema in the JAM-A$^{-/-}$ animals suggests less endothelial leakiness; however, we also observed less ulceration and a prominent epithelial regenerative response characterized by an increase in goblet cells (Fig. 4 F).

Increased intestinal epithelial cell proliferation in JAM-A$^{-/-}$ mice

Given the regenerative phenotype observed in the colonic mucosa of DSS-treated JAM-A$^{-/-}$ mice, we assessed epithelial proliferation in adjacent mucosal sections. Segments of the distal colon of control and JAM-A$^{-/-}$ mice were stained for Ki-67, a nuclear protein preferentially expressed during active phases of the cell cycle (G_1, S, G_2, and M phases) that is absent in resting (G_0) cells (25). Proliferating Ki-67–staining epithelial cells are normally restricted to the crypt region, as is seen in Fig. 5 A for control mice. However, in JAM-A$^{-/-}$ mice, Ki-67 staining extends from crypts toward the lumen along the normally quiescent crypt-to-surface axis (Fig. 5 A). Immunolabeling of colonic mucosal sections for the epithelial-specific marker β-catenin demonstrated that the Ki-67 cells were epithelial cells (Fig. 5 B). Similar increases in BrdU labeling were observed in JAM-A$^{-/-}$ colonic mucosa (unpublished data). In DSS-treated WT mice, Ki-67 staining was decreased compared with controls but was still increased in JAM-A$^{-/-}$ mice treated with DSS. However, Ki-67 staining levels did not appear to be increased above the untreated values in JAM-A$^{-/-}$ animals, suggesting altered regulation of proliferative responses (Fig. 5 B). It is possible that enhanced proliferation in JAM-A$^{-/-}$ animals results in a more rapid filling of epithelial defects and, hence, the improved histology scores observed in DSS-exposed JAM-A$^{-/-}$ mice.

In summary, these findings provide direct evidence for JAM-A–mediated regulation of intestinal epithelial barrier function through claudin expression and proliferation that, in

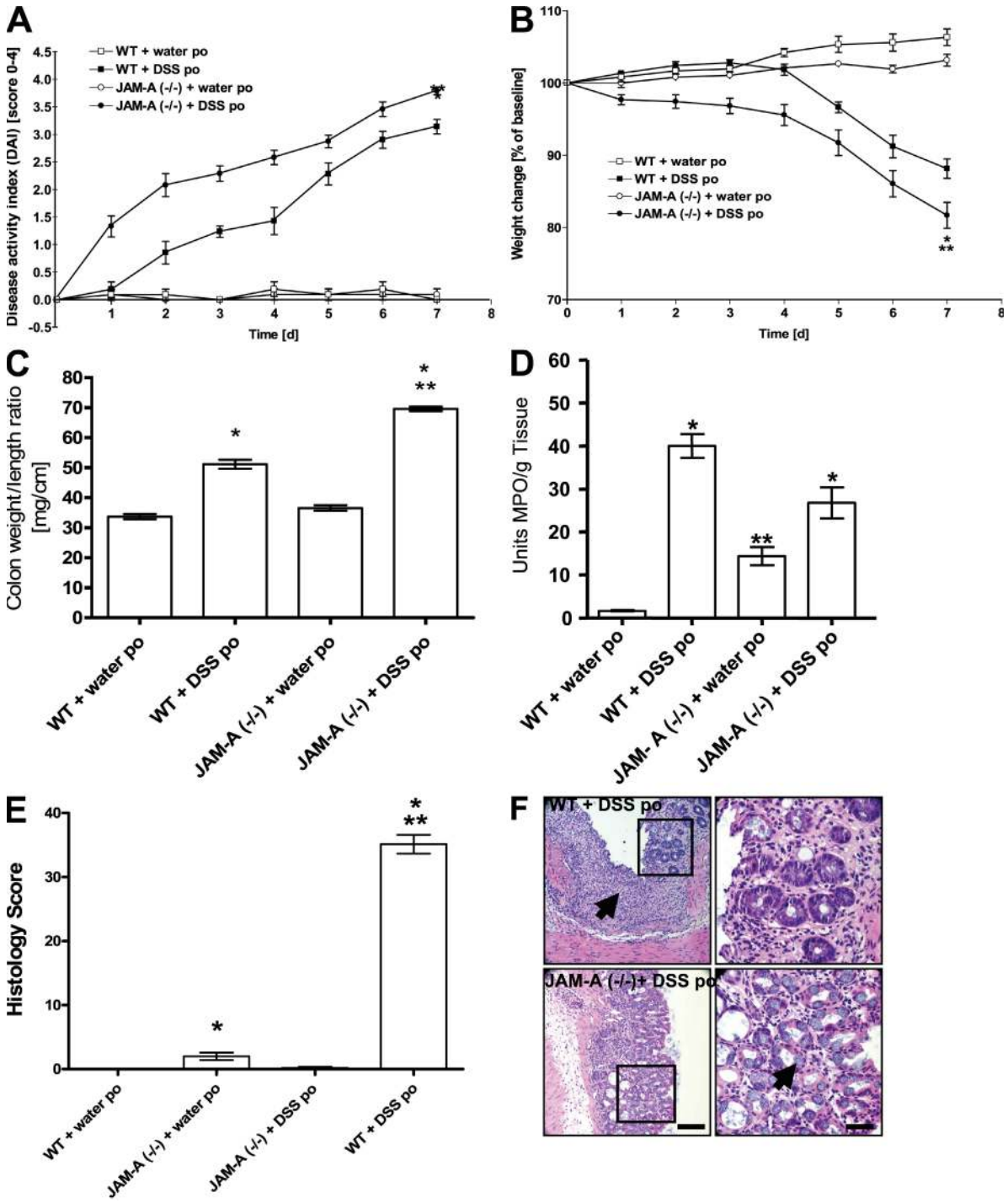

Figure 4. JAM-A deficiency increases susceptibility to DSS-induced colitis. (A) DAI. *, $P < 0.05$, increase in DSS treatment compared with mice plus water per os (po) beginning at day 2; **, $P < 0.05$, increase in JAM-A plus DSS treatment compared with WT and $JAM^{+/-}$ plus DSS starting at day 2. (B) Percent weight change. *, $P < 0.05$, DSS treatment compared with mice plus water po; **, $P < 0.05$, JAM-A plus DSS treatment compared with WT and $JAM^{+/-}$ plus DSS. (C) Colon weight/length ratio. *, $P < 0.05$ versus control mice; **, $P < 0.05$ versus WT plus DSS po. (D) Colonic MPO activity. *, $P < 0.05$ versus mice plus water po; **, $P < 0.05$ versus WT control mice. (E) Histology score. *, $P < 0.05$ versus water po; **, $P < 0.05$ versus WT plus DSS po. Error bars represent the mean ± SEM. (F) Colonic hematoxylin and eosin staining. Note the less crypt injury/ulceration and the abundance of goblet cells in JAM-$A^{-/-}$ mice compared with control (arrows). Bars: (left) 250 μm; (right) 50 μm.

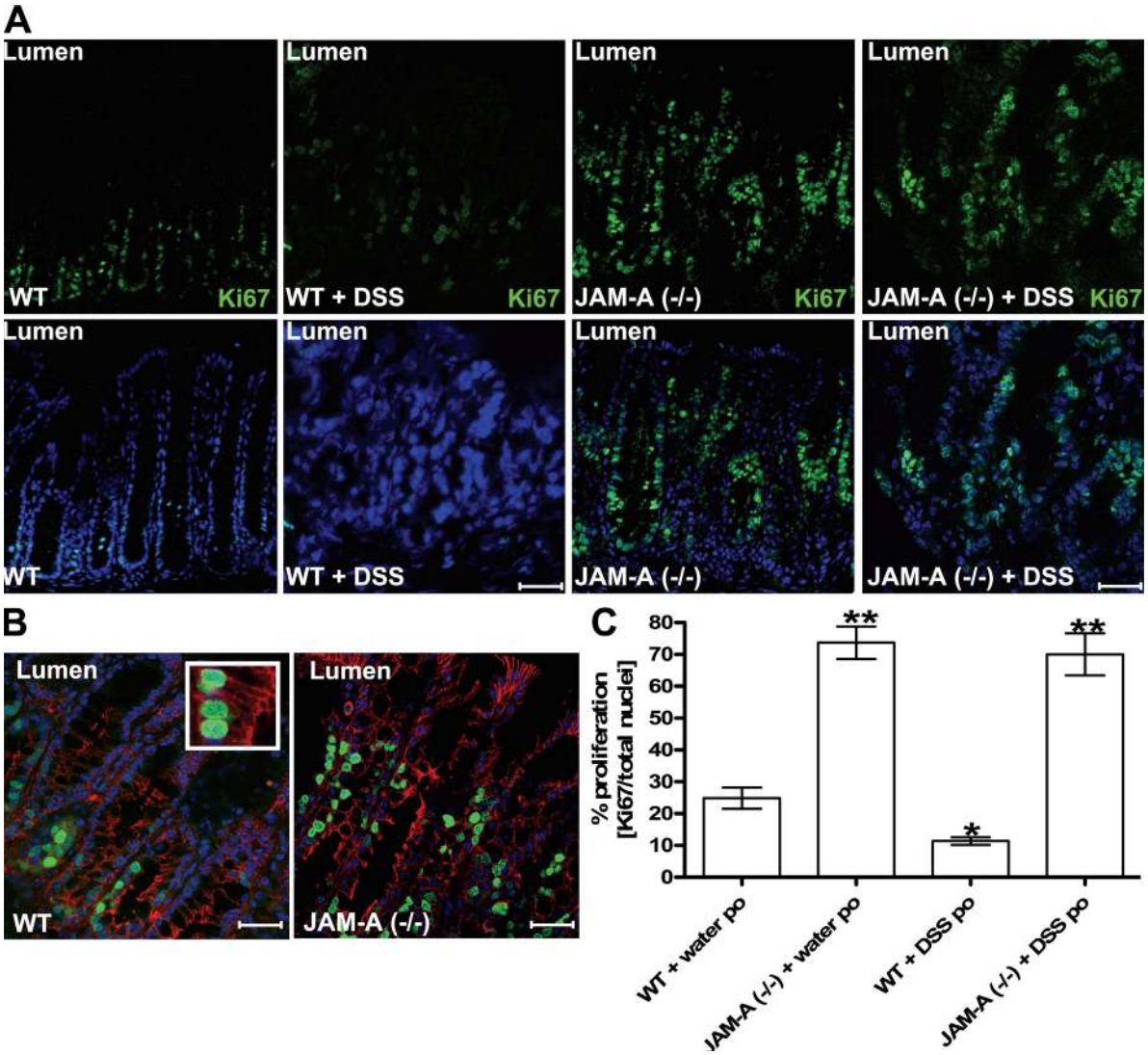

Figure 5. Increased epithelial proliferation in the colonic mucosa of JAM-A$^{-/-}$ mice. (A) Immunofluorescence labeling profile for Ki-67 in JAM-A$^{-/-}$ and WT mice before and after treatment with DSS. Ki-67 is shown in green and nuclei are shown in blue. (B) Ki-67–positive cells (green) costained with the epithelial cell marker β-catenin (red) and cell nuclei (blue). The inset highlights individual Ki-67–positive epithelial cells. Bars, 40 μM. (C) Analysis of the percentage of proliferating epithelial cells (three tissue sections stained per animal; $n = 5$ per group; *, $P < 0.05$. Error bars represent the mean ± SEM.

turn, regulates mucosal inflammation and responses to acute epithelial injury. More work is needed to determine the molecular basis of JAM-A regulation of TJ function and cellular proliferation and differentiation. Furthermore, given the observed differential epithelial and inflammatory responses to acute colonic injury in JAM-A$^{-/-}$ mice, studies with tissue-targeted deletion of JAM-A may help to delineate the mechanisms of JAM-A function in various cells and tissues.

MATERIALS AND METHODS

Cell culture, transfection, and immunoblotting. SK-CO15 human colonic epithelial cell lines were cultured as previously described (8). For siRNA transfection, siRNA (siGENOME SMARTpool) for human JAM-A, cyclophilin B, and a scramble control were purchased from Dharmacon. Each transfection was performed at least three times. SK-CO15 monolayers were scraped into a standard lysis buffer containing 1% TX-100 and a protease inhibitor cocktail (1:100; Sigma-Aldrich). PAGE and immunoblotting were conducted by standard protocol with 10–20 μg of total equalized protein.

Antibodies. Primary antibody suppliers were as follows: β-catenin, occludin, claudin-1, claudin-2, claudin-5, claudin-10, claudin-15, and anti–human JAM-A (Invitrogen); goat-biotinylated polyclonal antibody against mouse JAM-A (R&D Systems); and fluorophore-conjugated secondary antibodies (Alexa dyes; Invitrogen). Horseradish peroxidase (HRP)–conjugated secondary antibodies were purchased from Jackson ImmunoResearch Laboratories. HRP-conjugated streptavidin was obtained from Invitrogen. Both claudin-10 and -15 have two isoforms, both of which are recognized by the antibodies used.

Mice. All experimental protocols used either C57BL/6 (WT) mice (The Jackson Laboratory) or JAM-A$^{-/-}$ mice (a gift from T. Sato, Cornell University, New York, NY) and littermate controls, respectively. JAM-A$^{-/-}$ mice were produced as previously described (10) and were backcrossed for

seven generations on a C57BL/6 background strain obtained from the Jackson Laboratory. Disruption of the JAM-A gene was confirmed via PCR using primers designed to specifically detect hetero- and homozygote mice. All data represent results of two independent series of experiments with at least five mice (20–25 g) per group, unless otherwise indicated. All procedures using animals were reviewed and approved by the Emory University Institutional Animal Care and Use Committee and were performed according to National Institutes of Health criteria.

Induction of mouse colitis and harvest of colonic tissue. Mice were fed 5% (wt/vol) DSS (molecular mass = 36–50 kD; MP Biomedicals) dissolved in water for 7 d (24). Mice were killed at day 7, and colons were assessed for weight, length, MPO, and histology (see Histology). Analyses were performed on colonic segments located distal to the cecum. Colon samples were derived by dividing the distal colonic segment into three equal sections. Each section was analyzed for MPO and histology in adjacent tissue slices, as described.

Assessment of clinical disease in DSS-treated mice. Daily clinical assessment of DSS-treated animals included measurement of a validated clinical DAI ranging from 0 to 4, which was calculated using the following parameters: stool consistency, presence or absence of fecal blood, and weight loss (24).

Histology. For each animal, histological examination was performed on three segments of the distal colon. Adjacent tissue samples were processed for immunohistochemistry and stored at −80°C. Histological parameters were quantified in a blinded fashion using modified validated scoring systems (26, 27). Six independent parameters were measured: (a) severity of inflammation; (b) depth of injury; (c) crypt damage; (d) submucosal edema; (e) PMN in the lamina propria; and (f) mean number of goblet cells. Histological scores were multiplied by a factor reflecting the percentage of tissue involvement (×1, 0–25%; ×2, 26–50%; ×3, 51–75%; and ×4, 76–100%), and values were added to obtain a total score.

Immunohistochemistry. 5-μm cryo tissue sections were washed, fixed/permeabilized in absolute ethanol at −20°C for 20 min, blocked in $HBSS^+$ containing 5% normal goat serum for 1 h at room temperature, and incubated for 1 h with primary antibodies, followed by incubation with labeled secondary antibodies and final incubation with TO-PRO-3 iodide (Invitrogen) to visualize nuclei. Immunofluorescence images obtained on a confocal microscope (LSM 510; Carl Zeiss, Inc.) are representative of at least three experiments with multiple images taken per slide.

Western blot of intestinal mucosa. Intestinal mucosal cell lysates were prepared after the serosa and external longitudinal layer of the muscularis propria were stripped away. Isolated mucosal sheets were solubilized in SDS sample buffer and analyzed for claudin family members by Western blot. Band intensities for each sample were normalized with respect to actin loading controls, and data were reported as the JAM-$A^{-/-}$ sample band intensity divided by the WT sample band intensity.

Tissue MPO activity. MPO was measured in each of three distal colonic segments per mouse. Samples were rinsed with cold PBS, blotted dry, frozen in liquid nitrogen, and stored at −80°C until assay for MPO activity using the *o*-dianisidine method.

Analysis of claudin distribution. Fluorescence images were analyzed using image analysis software (LSM 510 META, version 4.2; Carl Zeiss, Inc.). Each analysis was performed in triplicate from each tissue section on a total of 10 images per mouse sample ($n = 5$).

In vivo permeability measurements across colonic mucosa. Intestinal permeability was assessed in vivo in mice using an FITC-labeled dextran (FD4; Sigma-Aldrich) method, as described previously (28).

Ussing chamber studies. Distal colonic mucosal sheets were harvested and mounted in dual channel Ussing chambers (U-2500; Warner Instruments, Inc.), as previously described (29). Samples were mounted between the two halves of the Ussing chamber (1.12-cm^2 opening). The mucosal and serosal sides of chambers (5ml vol) were connected to circulating reservoirs containing 37°C Ringer's solution and 5 mM mannitol. A gas lift column of 95% O_2, 5% maintained oxygenation and pH 7.4 of the reservoirs. I_{sc} was continuously monitored on a strip chart recorder, and electrical resistance ($\Omega \times cm^2$) was calculated using Ohm's law from ΔV and I_{sc}. After baseline potential difference and resistance were measured, 4-kD FITC-dextran (Sigma-Aldrich) was added to the mucosal side of the Ussing chamber to achieve a final concentration of 0.01 mM. Permeability was determined after removal of medium from serosal compartments at the end of the 180-min experimental period and assessed for fluorescence in a microplate fluorescence reader (FL-500; BIO-TEK) at an excitation wavelength of 485 nm and an emission wavelength of 530 nm.

Data analysis. Results are expressed as means ± SEM. p-values were calculated using a multifactorial analysis of variance test and an independent *t* test. $P < 0.05$ was considered significant.

The authors thank Dr. T. Sato for providing JAM-$A^{-/-}$ mice, Dr. C. Gonzales-Islas for assistance with Ussing chambers, and Dr. T. Denning for guidance performing flow cytometry.

This work was supported by grants from the German Research Foundation (DFG La 2359/1-1 to M.G. Laukoetter), the National Institutes of Health (DK72564, DK61379, and HL72724 to C.A. Parkos; DK55679 and DK59888 to A. Nusrat; DK64399 and R37 AI38296 to T.S. Dermody; T32 CA09385 to J.A. Campbell; and T32 DK007771 to C.T. Capaldo and E. Peatman), and the Crohn's and Colitis Foundation of America (P. Nava).

The authors have no conflicting financial interests.

Submitted: 11 July 2007
Accepted: 2 November 2007

REFERENCES

1. Olson, T.S., B.K. Reuter, K.G. Scott, M.A. Morris, X.M. Wang, L.N. Hancock, T.L. Burcin, S.M. Cohn, P.B. Ernst, F. Cominelli, et al. 2006. The primary defect in experimental ileitis originates from a nonhematopoietic source. *J. Exp. Med.* 203:541–552.
2. Jump, R.L., and A.D. Levine. 2004. Mechanisms of natural tolerance in the intestine: implications for inflammatory bowel disease. *Inflamm. Bowel Dis.* 10:462–478.
3. Peeters, M., B. Geypens, D. Claus, H. Nevens, Y. Ghoos, G. Verbeke, F. Baert, S. Vermeire, R. Vlietinck, and P. Rutgeerts. 1997. Clustering of increased small intestinal permeability in families with Crohn's disease. *Gastroenterology.* 113:802–807.
4. Schmitz, H., C. Barmeyer, M. Fromm, N. Runkel, H.D. Foss, C.J. Bentzel, E.O. Riecken, and J.D. Schulzke. 1999. Altered tight junction structure contributes to the impaired epithelial barrier function in ulcerative colitis. *Gastroenterology.* 116:301–309.
5. Martin-Padura, I., S. Lostaglio, M. Schneemann, L. Williams, M. Romano, P. Fruscella, C. Panzeri, A. Stoppacciaro, L. Ruco, A. Villa, et al. 1998. Junctional adhesion molecule, a novel member of the immunoglobulin superfamily that distributes at intercellular junctions and modulates monocyte transmigration. *J. Cell Biol.* 142:117–127.
6. Rehder, D., S. Iden, I. Nasdala, J. Wegener, M.K. Brickwedde, D. Vestweber, and K. Ebnet. 2006. Junctional adhesion molecule-a participates in the formation of apico-basal polarity through different domains. *Exp. Cell Res.* 312:3389–3403.
7. Babinska, A., M.H. Kedees, H. Athar, T. Ahmed, O. Batuman, Y.H. Ehrlich, M.M. Hussain, and E. Kornecki. 2002. F11-receptor (F11R/JAM) mediates platelet adhesion to endothelial cells: role in inflammatory thrombosis. *Thromb. Haemost.* 88:843–850.
8. Mandell, K.J., B.A. Babbin, A. Nusrat, and C.A. Parkos. 2005. Junctional adhesion molecule 1 regulates epithelial cell morphology through effects on beta1 integrins and Rap1 activity. *J. Biol. Chem.* 280:11665–11674.
9. Naik, M.U., S.A. Mousa, C.A. Parkos, and U.P. Naik. 2003. Signaling through JAM-1 and alphavbeta3 is required for the angiogenic action

of bFGF: dissociation of the JAM-1 and alphavbeta3 complex. *Blood*. 102:2108–2114.
10. Cera, M.R., A. Del Prete, A. Vecchi, M. Corada, I. Martin-Padura, T. Motoike, P. Tonetti, G. Bazzoni, W. Vermi, F. Gentili, et al. 2004. Increased DC trafficking to lymph nodes and contact hypersensitivity in junctional adhesion molecule-A-deficient mice. *J. Clin. Invest.* 114:729–738.
11. Kang, L.I., Y. Wang, A.T. Suckow, K.J. Czymmek, V.G. Cooke, U.P. Naik, and M.K. Duncan. 2007. Deletion of JAM-A causes morphological defects in the corneal epithelium. *Int. J. Biochem. Cell Biol.* 39:576–585.
12. Van Itallie, C.M., and J.M. Anderson. 2006. Claudins and epithelial paracellular transport. *Annu. Rev. Physiol.* 68:403–429.
13. Furuse, M., K. Furuse, H. Sasaki, and S. Tsukita. 2001. Conversion of zonulae occludentes from tight to leaky strand type by introducing claudin-2 into Madin-Darby canine kidney I cells. *J. Cell Biol.* 153:263–272.
14. Carrozzino, F., P. Soulie, D. Huber, N. Mensi, L. Orci, A. Cano, E. Feraille, and R. Montesano. 2005. Inducible expression of Snail selectively increases paracellular ion permeability and differentially modulates tight junction proteins. *Am. J. Physiol. Cell Physiol.* 289:C1002–C1014.
15. Van Itallie, C., C. Rahner, and J.M. Anderson. 2001. Regulated expression of claudin-4 decreases paracellular conductance through a selective decrease in sodium permeability. *J. Clin. Invest.* 107:1319–1327.
16. Fleming, T.J., M.L. Fleming, and T.R. Malek. 1993. Selective expression of Ly-6G on myeloid lineage cells in mouse bone marrow. RB6-8C5 mAb to granulocyte-differentiation antigen (Gr-1) detects members of the Ly-6 family. *J. Immunol.* 151:2399–2408.
17. Corada, M., S. Chimenti, M.R. Cera, M. Vinci, M. Salio, F. Fiordaliso, N. De Angelis, A. Villa, M. Bossi, L.I. Staszewsky, et al. 2005. Junctional adhesion molecule-A-deficient polymorphonuclear cells show reduced diapedesis in peritonitis and heart ischemia-reperfusion injury. *Proc. Natl. Acad. Sci. USA.* 102:10634–10639.
18. Mandell, K.J., G.P. Holley, C.A. Parkos, and H.F. Edelhauser. 2006. Antibody blockade of junctional adhesion molecule-A in rabbit corneal endothelial tight junctions produces corneal swelling. *Invest. Ophthalmol. Vis. Sci.* 47:2408–2416.
19. Colegio, O.R., C.M. Van Itallie, H.J. McCrea, C. Rahner, and J.M. Anderson. 2002. Claudins create charge-selective channels in the paracellular pathway between epithelial cells. *Am. J. Physiol. Cell Physiol.* 283:C142–C147.
20. Van Itallie, C.M., S. Rogan, A. Yu, L.S. Vidal, J. Holmes, and J.M. Anderson. 2006. Two splice variants of claudin-10 in the kidney create paracellular pores with different ion selectivities. *Am. J. Physiol. Renal Physiol.* 291:F1288–F1299.
21. Tsukita, S., M. Furuse, and M. Itoh. 2001. Multifunctional strands in tight junctions. *Nat. Rev. Mol. Cell Biol.* 2:285–293.
22. Olson, T.S., G. Bamias, M. Naganuma, J. Rivera-Nieves, T.L. Burcin, W. Ross, M.A. Morris, T.T. Pizarro, P.B. Ernst, F. Cominelli, and K. Ley. 2004. Expanded B cell population blocks regulatory T cells and exacerbates ileitis in a murine model of Crohn's disease. *J. Clin. Invest.* 114:389–398.
23. Kawamura, T., T. Kanai, T. Dohi, K. Uraushihara, T. Totsuka, R. Iiyama, C. Taneda, M. Yamazaki, T. Nakamura, T. Higuchi, et al. 2004. Ectopic CD40 ligand expression on B cells triggers intestinal inflammation. *J. Immunol.* 172:6388–6397.
24. Krieglstein, C.F., W.H. Cerwinka, A.G. Sprague, F.S. Laroux, M.B. Grisham, V.E. Koteliansky, N. Senninger, D.N. Granger, and A.R. de Fougerolles. 2002. Collagen-binding integrin alpha1beta1 regulates intestinal inflammation in experimental colitis. *J. Clin. Invest.* 110:1773–1782.
25. Scholzen, T., and J. Gerdes. 2000. The Ki-67 protein: from the known and the unknown. *J. Cell. Physiol.* 182:311–322.
26. Dieleman, L.A., M.J. Palmen, H. Akol, E. Bloemena, A.S. Pena, S.G. Meuwissen, and E.P. Van Rees. 1998. Chronic experimental colitis induced by dextran sulphate sodium (DSS) is characterized by Th1 and Th2 cytokines. *Clin. Exp. Immunol.* 114:385–391.
27. Barthel, M., S. Hapfelmeier, L. Quintanilla-Martinez, M. Kremer, M. Rohde, M. Hogardt, K. Pfeffer, H. Russmann, and W.D. Hardt. 2003. Pretreatment of mice with streptomycin provides a *Salmonella enterica* serovar Typhimurium colitis model that allows analysis of both pathogen and host. *Infect. Immun.* 71:2839–2858.
28. Napolitano, L.M., M.J. Koruda, A.A. Meyer, and C.C. Baker. 1996. The impact of femur fracture with associated soft tissue injury on immune function and intestinal permeability. *Shock.* 5:202–207.
29. Madara, J.L. 1983. Increases in guinea pig small intestinal transepithelial resistance induced by osmotic loads are accompanied by rapid alterations in absorptive-cell tight-junction structure. *J. Cell Biol.* 97:125–136.